Session VI, September 19, Thursday

L19

ROTAČNĚ KOVANÁ MĚĎ

Kopeček J.[1], Kmječ T.[1], Mestek S.[1], Veřtát P.[1], Šimek D.[1], Ahmed U.[1], M. Benč[2], J. Walek[2], Kunčická L.[2], Kocich R.[2]

[1]FZU – Institute of Physics of the Czech Academy of Sciences, Praha, Czech Republic
[2]Faculty of Materials Science and Technology, VŠB–Technical University of Ostrava, Ostrava-Poruba, Czech Republic

Měď vyniká výtečnou elektrickou vodivostí, ale její mechanické vlastnosti nejsou valné [1]. Když jsou pak zlepšeny, například příměsemi, dochází k rapidnímu snížení vodivosti, protože příměsové atomy, či částice, které je obsahují, rozptylují vodivostní elektrony. Vcelku překvapivou metodou řešení tohoto dilematu se ukázaly některé metody značné plastické deformace, které vytvářejí velké množství nanodvojčat [2]. V takto připravených vzorcích byla pozorována větší vodivost než v konvenčně žíhané mědi. Předpokládáme, že dvojčatové hranice, jako příklad speciálních hranic s velmi malou přebytečnou energií vrstevné poruchy, působí jako kanály, které vedou elektrický proud téměř bezrozptylově. Samozřejmě jiné poruchy, jako jsou obecné hranice zrn nebo dislokace elektrony rozptylují a zvyšují elektrický odpor, což vede k ohřevu materiálu a degradaci mechanických vlastností.

Koncept tvorby velkého množství nanodvojčat je stále živý a dále rozpracovávaný pro různé materiály i po dvaceti letech od svého objevu [3]. V naší práci byl nejprve studován čistý materiál kovaný při teplotě kapalného dusíku, nyní jsme využili komerčně čistou s přídavkem 1 % Al_2O_3, která byla rotačně kována (RS) při pokojové teplotě v zařízení Komafu S600, při využití zkušeností členů týmu s metodikou RS [5-6]. Materiál byl míchán a následně v měděné trubce kompaktizován kováním při redukci z 50 mm na průměry 13 a 10 mm. Vykované tyče byly dále žíhány a všechny stavy byly standardně zkoumány pomocí SEM (Tescan FERA 3), EDS a EBSD (EDAX Octane super 60 mm^2 a Digiview IV), TEM (Jeol JEOL 2000 FX) a XRD (Panalytical X´Pert).

Potvrdili jsme, že rotační kování při teplotě kapalného dusíku vytváří silnou texturu ve směru 111 v ose kování, složka ve směru 100 je oproti čistému materiálu výrazně slabší. Zrna jsou ve směru osy tyče protažena, ale jsou významně kratší než v kovaném materiálu. Po žíhání tato mikrostruktura rekrystalizuje, vodivost roste, avšak zůstává nižší než 100 % IACS. Snížení vodivosti oproti hodnotě IACS je dáno obsahem Al_2O_3, a tedy rozptylem vodivostních elektronů na částicích v matrici. Pomocí TEM byly pozorovány dislokační stěny. Předpokládáme, že pozorování poruch krystalové mříže je ovlivněno schopností mědi relaxovat i v nízkých teplotách [7], ale není zcela řízeno rychlými procesy při přípravě.

1. J. R. Davies (Ed), ASM Specialty Handbook, Copper and Copper Alloys, Materials Park, ASM International, 2001.
2. L. Lu, Y.F. Shen, X.H. Chen, L.H. Qian, K. Lu, Ultrahigh strength and high electrical conductivity in copper, Science, 304 (2004), 422-426.
3. X. Ke, J. Ye, Z. Pan, J. Geng, M.F. Besser, D. Qu, A. Caro, J. Marian, R.T. Ott, Y.M. Wang, F. Sansoz, Ideal maximum strengths and defect-induced softening in nanocrystalline-nanotwinned metals, Nature Materials, 18 (2019), 1207-1214.
4. Kopeček J., Bajtošová L., Veřtát P., Šimek D., *(Sub)structure Development in Gradually Swaged Electroconductive Bars*, Materials, 16 (2023) 5324-1 – 5324-12.
5. P. Strunz, L. Kunčická, P. Beran, R. Kocich, Ch. Hervoches, Correlating Microstrain and Activated Slip Systems with Mechanical Properties within Rotary Swaged WNiCo Pseudoalloy, Materials, 13(2020), 208.
6. D. Canelo-Yubero, R. Kocich, J. Šaroun, P. Strunz, Residual Stress Distribution in a Copper-Aluminum Multifilament Composite Fabricated by Rotary Swaging, Materials, 16 (2023), 2102.
7. Král P., Staněk J., Kunčická L., Seitl F., Petrich L., Schmidt V., Beneš V., Sklenička V.: Microstructure changes in HPT-processed copper occurring at room temperature. Mater. Character. 151 (2019) 602-611.

We acknowledge Czech Science Foundation project 22-11949S and CzechNanoLab Research Infrastructure (LM2023051) by MEYS CR for support.

L19

Ion implantation of titanium alloys
IONTOVÁ IMPLANTACE TITANOVÝCH SLITIN

J. Drahokoupil[1,2,3], M. Lebeda[1,2,3],P. Hruška[1], J. Kopeček[1], A. Školáková[1], P. Vlčák[3]

[1]Fyzikální ústav, Akademie věd České Republiky, Na Slovance 2, 182 21 Praha 8, Česká Republika
[2]Katedra inženýrství pevných látek, Fakulta jaderná a fyzikálně inženýrská v Praze, České vysoké učení technické v Praze, Technická 4, 166 07 Praha 6 - Dejvice, Česká Republika
[3]Ústav fyziky, Fakulta strojní, České vysoké učení technické v Praze, Technická 4, 166 07 Praha 6 - Dejvice, Česká Republika
draho@fzu.cz

Titan a jeho slitiny jsou hojně používány v leteckém, automobilovém a chemickém průmyslu a nacházejí také široké uplatnění v biomedicínských aplikacích. Důvodem je jejich vysoká pevnost v tahu, dobrá korozní a únavová odolnost, tvárnost, relativně nízký modul pružnosti a výjimečná biokompatibilita a biologická neutralita. Nevýhodou titanu a titanových slitin pro některé aplikace je však jejich špatné chování v tahu, nedostatečná povrchová tvrdost a špatná odolnost vůči některým chemickým prostředím. Z tohoto důvodu je nutno pro mnohé aplikace povrch titanových materiálů modifikovat. V popředí našeho zájmu stojí iontová implantace dusíku. Ukazuje se, že tato metoda značně zlepšuje mechanické vlastnosti a zátěžovou a korozní odolnost velké skupiny materiálů (kovů, polymerů a keramik). Ovlivněná hloubka iontovou implantací dosahuje pouze několika stovek nanometrů. Při iontové implantaci dusíku menšími dávka do titanu dochází postupnému k nárůstu mřížkových parametrů původní hexagonální struktury. S rostoucí dávkou pak dochází tvorbě kubické TiN fáze. Pokod budeme s implantací nadále pokračovat, začnou se oběvovat puchářky a prasklinky, s ještě větší dávkou se pak puchářky odlupují a odhalují porézní strukturu TiN

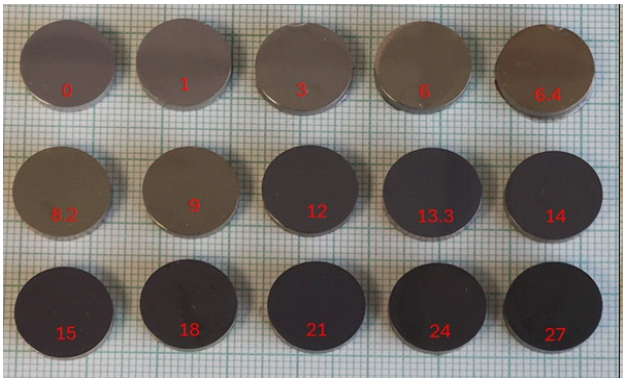

Obrázek 1. Fotka dusíkem implanovaných vzorků titanu. Číslo na vzorku značí dávku v jednotkách 10^{17} iontů N/cm^2.

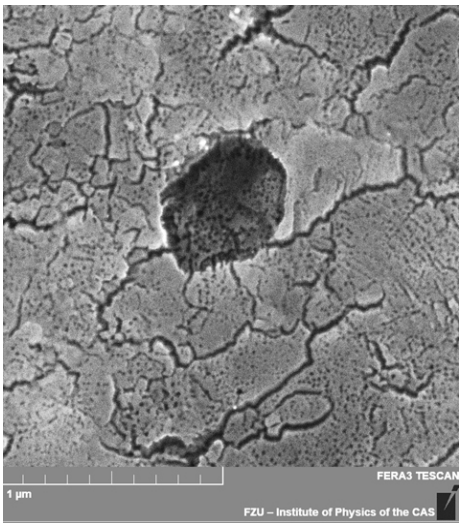

Obrázek 2. Povrch titanové vzorku implantovaného s fluencí dusíku $27 \cdot 10^{17}$ cm^{-2}.

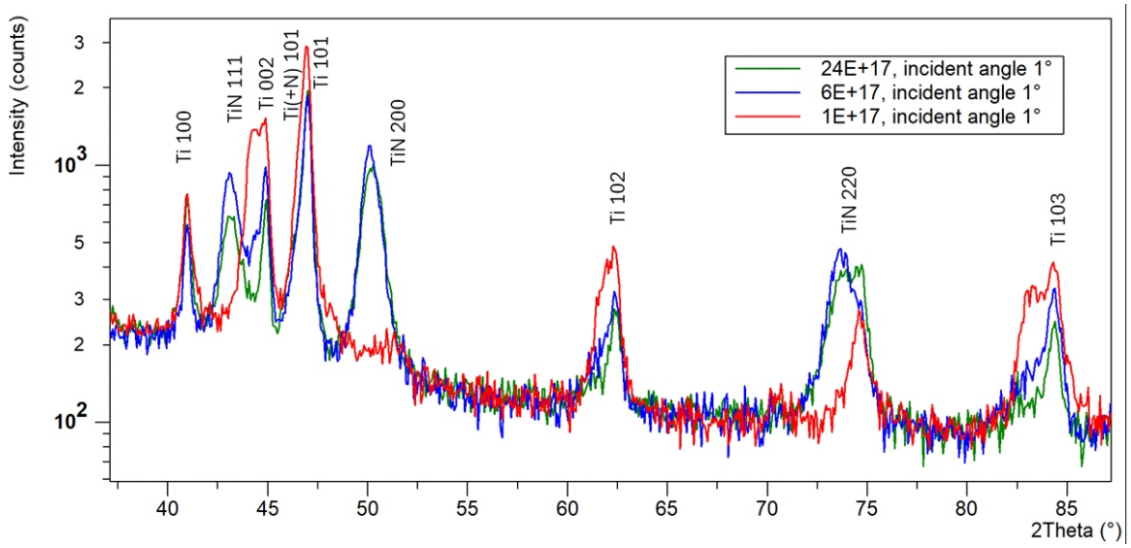

Obrázek 3. Difrakční záznamy implantovaných titanových vzorků s různou implantovanou dávkou dusíku.

(obr 2). Na obr. 1 je fotografie povrchů sady vzorků titanu (Ti grade II) s různou implantovanou dávkou pod $1E^{+17}$ po $27E^{+17}$ inotnů dusíku na cm^2. Je patrné, že s rostoucí dávkou povrch vzorku postupně zlátne (TiN fáze) a pak začne díky poréznímu povrchu viditelně tmavnout.

Difrakční analýza je komplikována zejména tloušťkou ovlivněné vrstvy, která je v malých stovkách nm, přičmž maximální koncentrace dusíku bývá v hloubce cca 80 nm a také nehomogenitou celé vrstvy. Fáze TiN s menší koncentrací dusíku má menší mřížkové parametry. A obdobně mřížkový parametr hexagonální původně titanové struktury se zvetšuje s rostoucí koncentrací dusíku. Výsledné difrakční záznamy jsou tedy váženou sumou všech přítomných fází s jejich proměnou koncentrací což se projevuje rozšířením difrakčních maxim.

L20

INTERNAL NITRIDING OF HIGH ENTROPY ALLOYS

F. Lukáč[a,d], M. Klementová[b], M. La[c], L. Cvrček[c], P. Minárik[d], J. Kozlík[d]

[a]*Institute of plasma physics, Czech Republic*
[b]*Institute of Physics of the Czech Academy of Sciences, Czech Republic*
[c]*Faculty of Mechanical Engineering, Czech Technical University in Prague, Czech Republic*
[d]*Mathematics and physics faculty, Charles University in Prague, Czech Republic*
lukac@ipp.cas.cz

Spark plasma sintering (SPS) is a well-recognized method in powder metallurgy which produces ultra fine grained materials with outstanding properties. Short times are sufficient for mutual appliance of pressure and temperature during powder sintering and simultaneously the grain growth is significantly reduced. This highly depends on the homogeneity, purity and size distribution of powder feedstock. In our study, high energy milling in various atmospheres was used to prepare HfNbTaTiZr powders and phase composition of sintered materials was investigated providing huge impact on material properties. It was found to be the formation of very fine microstructure of interconnected BCC phase and unexpected FCC phase, see Figure 1. Detailed TEM investigation revealed that the formation of ZrHfTi-rich oxo-nitrites has taken place during sintering of powders milled in air or in oxygen atmosphere [1]. Correlation of oxygen and nitrogen content with FCC phase volume was investigated. The Rietveld refinement analysis coupled with whole powder pattern modelling was performed. It provided the essential information about the phase fractions and stoichiometry of $ZrHfTi(O,N)_x$ complexes. Promising mechanical properties like very high hardness and high temperature wear resistance were tested.

1. Lukáč, F et al.: The origin and the effect of the fcc phase in sintered HfNbTaTiZr, *Materials Letters*, 286, (2021), 129224, https://doi.org/10.1016/j.matlet.2020.129224.

This project is supported by Czech Science Foundation grant no. 22-24563S.

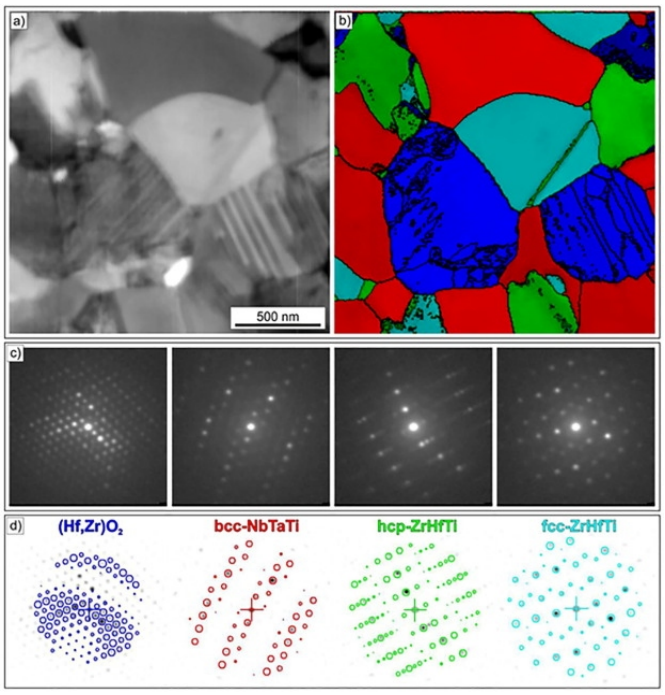

Figure 1. ACOM phase mapping. a) virtual BF image, b) phase map, c) experimental diffraction patterns (DP) and d) DPs overlaid with matching templates of the respective phases.

L21

RESIDUAL STRESSES, STRAIN, MORPHOLOGY AND ORIENTATION RELATION IN Cr AND Mo LAYERS DEPOSITED ON VARIOUS SUBSTRATES

Petr Cejpek, David Rafaja, Mykhaylo Motylenko, Christian Schimpf, Astrid Leuteritz, Shail Shah

Institute of Materials Science, TU Bergakademie Freiberg, Gustav-Zeuner-Str. 5, 09599 Freiberg, Germany

The study presented here is a part of the project focused on the fundamental description of the laser ablation process. The laser ablation could introduce craters into a material which can play an important role in a modification of local material properties, especially microstructure. The microstructural properties inside the craters could then work as *post mortem* probes of condition (temperature, pressure) during ablation itself.

However, to describe these microstructural changes properly, well known original state of a material is the necessary prerequisite. For this purpose, the 100 nm thick epitaxial layers of Cr and Mo were deposited by magnetron physical vapour deposition (PVD) on various substrates: amorphous SiO_2 and single-crystalline MgO(100), MgO (110) and corundum Al_2O_3(0001). The microstructural properties such as residual stresses, grain sizes, layer morphology and crystallographic orientation have been studied in the mean of the X-ray diffraction and electron microscopy.

With the use of an amorphous substrate SiO_2, both Cr and Mo layer grows with the 110 fibre texture. Here, the surface energy plays the decisive role, which is the lowest at 110 crystallographic plane (Cr and Mo are both bcc metals).

Using a single crystalline substrate, the minimalization of the deformation energy leading from the lattice misfit between the layer and substrate will play an important role. Therefore, deposited layers will grow in the specific orientation relation with the substrate. However, a presence of several variants with different orientation was observed in some cases. Individual orientation relations were deduced from the measured pole figures (example in **Figure 1a** and **1b**) and are shown in **Table 1**.

The residual stresses obtained by $\sin^2$ method are shown in **Table 1**. The results show, that the layers posses quite high residual stresses in the order of several GPa. In comparison to the yield strength (0.131 GPa for Cr and 0.324 GPa for Mo [1]), this points to a fact that there should be an inner mechanism leading to the material hardening. The analysis of the diffraction peaks broadening and also transmission electron microscopy show that the deposited layers consist of the small columnar crystallites with the size of d = 20-50 nm (see Figure **1c**). The presence of such crystallites leads to an increase of the yield strength through the Hall-Petch relation $_{yield}$ $d^{\frac{1}{2}}$ [2].

1. Theodore Gray, *Periodic Table (website)*, https://periodictable.com/, visited 8.8.2024
2. Niels Hansen, *Hall–Petch relation and boundary strengthening*, Scripta Materialia 51 (2004) 801–806, doi: 10.1016/j.scriptamat.2004.06.002.

Table 1: Out-of-plane orientation of studied layers and their residual lateral stress $_{lat}$.

		Substrate					
		MgO(100)		MgO(110)		Al_2O_3(0001)	
		out-of-plane orientation	$_{lat}$	out-of-plane orientation	$_{lat}$		$_{lat}$
layer	Cr	100	1.4	Twins with 211	4.2 3.8	unspecfied fiber texture	-
	Mo	100 and 2 variants with 110 (= 90°)	-1.5 -0.8 -0.8	Twins with 21	3.5 3.5	3 variants with 110 (= 60°)	1.5 1.5 1.4

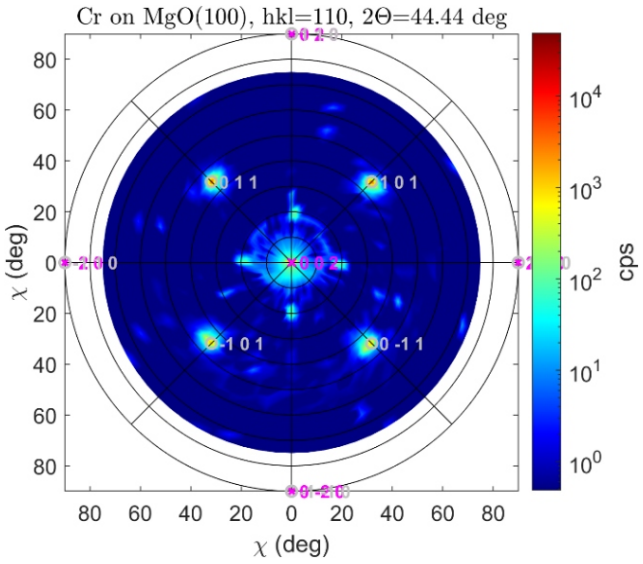

a)

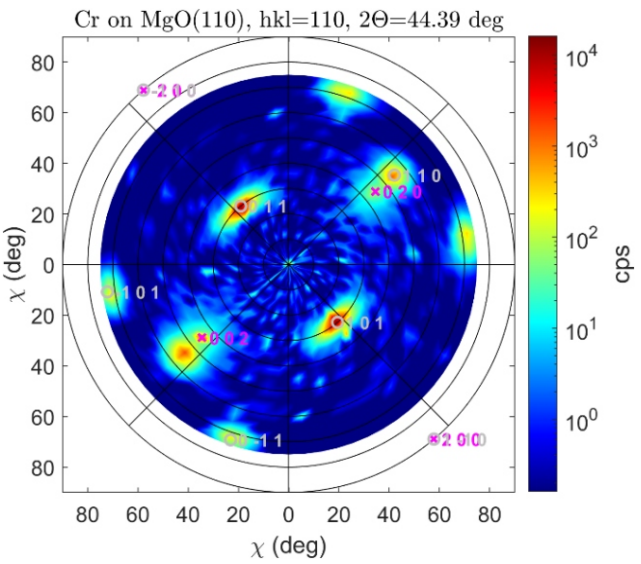

b)

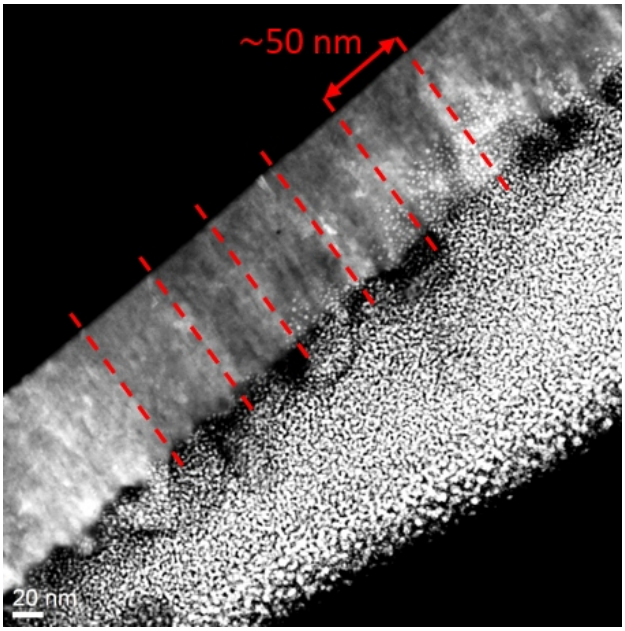

Figure 1. **a)** Pole figure 110 measured on Cr layer deposited on MgO(100) substrate, **b)** Pole figure 110 measured on Cr layer deposited on MgO(110) substrate. The purple crosses correspond to the simulated positions of substrate diffraction peaks, the gray crosses correspond to one of Cr variant (see Table 1).
c) (left) Dark field image measured by TEM showing the crystallites in Cr layer deposited on MgO(110) substrate.

L22

NIOBIUM NITRIDE THIN FILMS – CORRELATION OF ELECTRIC PROPERTIES TO STRUCTURE

T. Kosutova[1], Y. Yao[1], Z. Zhang[1], F. Gustavo[2], F. Lefloch[2], S.- L. Zhang[1], T. Kubart[1]

[1]Division of Solid-State Electronics, Department of Electrical Engineering, Uppsala University, Uppsala 751 03, Sweden

[2]Université Grenoble Alpes, CEA, Grenoble INP, IRIG, PHELIQS, 38000 Grenoble, France

tereza.kosutova@angstrom.uu.se

Niobium nitride in bulk form exhibits relatively high superconducting transition temperature (T_c), around 16 K. Therefore, it is intensively studied for applications such as qubits in quantum computing, infrared light detectors or superconducting radio frequency cavities in particle accelerators. The application fields can be further broadened by making the preparation of thin NbN films compatible with the CMOS process technology and using directly silicon wafers as a substrate; note that silicon is not inherently suitable for the growth of high-quality NbN due to the large lattice mismatch.

Our study aims to deposit thin films of NbN with sufficiently high T_c with a technique that is scalable to semiconductor industrial demands and has low thermal stress on the sample. In the first part of our study, we have identified stoichiometry and porosity as the most essential characteristics of the NbN thin films. They can be tuned by varying deposition parameters during the film preparation. Specifically, magnetron sputtering along with its ionized variant is shown to be a highly promising technical approach. In order to find the best deposition conditions, we have focused on increasing the density and conductivity of our 100-nm thick NbN films. These are found to be correlated to each other and significantly improved by using high-power impulse magnetron sputtering (HiPIMS) with the disadvantage of a somewhat lowered deposition rate.

In the second part of the study, the microstructure of the HiPIMS samples is characterized in detail and its influence on the superconducting transition temperature and width is analysed. The stoichiometry of the films, determined by the elastic recoil detection analysis in combination with X-ray reflectivity and X-ray diffraction, seems to be crucial for reaching high T_c. Also, decreasing internal stress and microstrain helps to increase T_c. On the contrary, the transition temperature is found not much dependent on the grain size.

Finally, our approach is found suitable for creating test circuits and device structures of dimensions on the order of hundreds of nanometers. These structures have been used in our critical current density measurements.

This project was funded within the QuantERA II Program through the Swedish Research Council (2021-06025) and the French National Research Agency (SUNISIDEuP – ANR-19-CE47-0010).

L23

STUDY OF TIN SURFACE

Pavla Roupcová, Oldřich Schneeweiss, Dinara Sobola, Martin Friák, Alena Michalcová

Brno University of Technology
Institute of Physics of Materials, Czech Academy of Sciences

The aim of our study is to analyze the surface of higher-temperature tetragonal (white) beta-tin, which tends to transform into stable alfa-tin (grey) under several conditions that have not yet been sufficiently explained. The beta-tin typically starts to transform upon cooling under 13.2°C, and its transformation rate accelerates with undercooling to its maximum at -53°C. But that process itself is taking an immensely long time (up to years). The transformation rate increases with the help of nucleation by alfa-tin particles (so-called inoculation) and pressure (resulting in a reduction of the transformation time to days and hours). The transformation also starts by helping the different types of compounds, e.g. CdTe, InSb, etc., and the pressure magnitude changes the transformation rate too. The surface of beta-tin is passivated by SnO the same way as the surface of Al and stainless steel by Al_xO_y and Cr_xO_y.

We study the very thin passivating oxide layer by different methods, which are more sensitive to the surface than X-ray powder diffraction (XRPD), e.g. GIXRD, CEMS, XPS and FTIR. The surface study shows the SnO could also be nuclei of the whole transformation process.

The financial support from the Czech Science Foundation received under Project No. 22-05801S is gratefully acknowledged.

L24

LATTICE DYNAMICS OF Y-KAPELLASITE

P. Doležal[1,2], T. Biesner[3], Y. Li[4,5], R. Mathew Roy[3], S. Roh[3], R. Valentí[4], M. Dressel[3], P. Puphal[6], A. Pustogow[2]

[1]Charles University, Faculty of Mathematics and Physics, Department of Condensed Matter Physics, Ke Karlovu 5, 121 16 Prague 2, Czech Republic
[2] Institute of Solid State Physics, TU Wien, Vienna 1040, Austria
[3]1. Physikalisches Institut, Universität Stuttgart, 70569 Stuttgart, Germany
[4]Institut für Theoretische Physik, Goethe-Universität Frankfurt, 60438 Frankfurt am Main, Germany
[5]MOE Key Laboratory for Nonequilibrium Synthesis and Modulation of Condensed Matter, School of Physics, Xi'an Jiaotong University, Xi'an 710049, China
[6] Max Planck Institute for Solid State Research, 70569 Stuttgart, Germany

Quantum Spin Liquid (QSL) is a ground state of condensed matter, which is characterized by the absence of magnetic order down to the lowest temperatures along with long-range entanglement of fluctuating spin excitations [1, 2]. Such a state of matter can be promoted by magnetic frustration which prevents the magnetic moments from antiferromagnetic ordering. Among lattices with a high degree of frustration belongs the kagome lattice. Such lattice can be found in herbertsmithite and other substituted compounds like our studied Y–kapellasite [3]. Here the kagome lattice is distorted and the compound has an antiferromagnetic transition at $T_N = 2.2$ K [4]. The dilatometry measurements show anomalous behaviour around 32 K, where the magnetic interactions are already significant [5]. The questions arise: Is there a structural transition? How big is magnetoelastic coupling and does it has a significant influence on the crystal lattice?

The previous single crystal X-ray and neutron diffraction were not conclusive about the crystal structure modification. The neutron diffraction were able to detect at T_s = 32 K an abrupt change in intensity of the (6 0 0) and (0 0 18) diffraction maxima. Therefore we focused on the lattice dynamics studied by infrared spectroscopy. The obtained results are compared with the *ab initio* calculations. The findings prove the lowering of the crystal lattice symmetry and suggest the key role of H atoms in the crystal structure modifications. The low-energy phonons exhibit significant softening, which can be a sign of enhanced magnetoelastic interactions.

1. Balents, L., *Spin liquids in frustrated magnets.* Nature, 2010. **464**(7286): p. 199-208.
2. Broholm, C., et al., *Quantum spin liquids.* Science, 2020. **367**(6475): p. 1-9.
3. Puphal, P., et al., *Kagome quantum spin systems in the atacamite family.* Physical Review Materials, 2018. **2**(6): p. 063402-1-11.
4. Puphal, P., et al., *Strong magnetic frustration in $Y_3Cu_9(OH)_{19}Cl_8$: a distorted kagome antiferromagnet.* Journal of Materials Chemistry C, 2017. **5**(10): p. 2629-2635.
5. Chatterjee, D., et al., *From spin liquid to magnetic ordering in the anisotropic kagome Y-kapellasite $Y_3Cu_9(OH)_{19}Cl_8$: A single-crystal study.* Physical Review B, 2023. **107**(12): p. 125156-1-13.

This work was supported by the Czech Science Foundation via research project GAČR 23-06810O.

L25

XRD STRUCTURAL STUDIES OF STRONGLY ORIENTED HEXAFERRITE THIN FILMS WITH POTENTIAL MAGNETOELECTRIC EFFECT PREPARED BY CHEMICAL SOLUTION DEPOSITION

R. Kužel[1], J. Buršík[2], M. Dopita[1], L. Horák[1], M. Soroka[2]

[1]Charles University, Faculty of Mathematics and Physics – Prague, Czech Republic
[2]Institute of Inorganic Chemistry of the Czech Academy of Sciences - Husinec-Rez, Czech Republic

Bulk hexaferrites are quite known to exhibit strong magnetoelectric (ME) effects near room temperature. However, in thin films the same effect have not often been realized. Our research has been concentrated on studies of different hexaferrite phases - M, Y, W, X, U and Z prepared by chemical solution deposition already for quite a long time. The phases are either hexagonal or trigonal and the crystal structure is typical by long unit cell and different stackings of basic building blocks. The ME effect was detected mainly in Y and Z films but other phases have been studied as well and in several cases they were prepared in a form of thin film for the first time [e.g. 1-4].

Chemical solution deposition method was applied, and several processing parameters were tested and optimized with the aim of minimizing the amount of impurities that could spoil the magnetic properties of the final material.

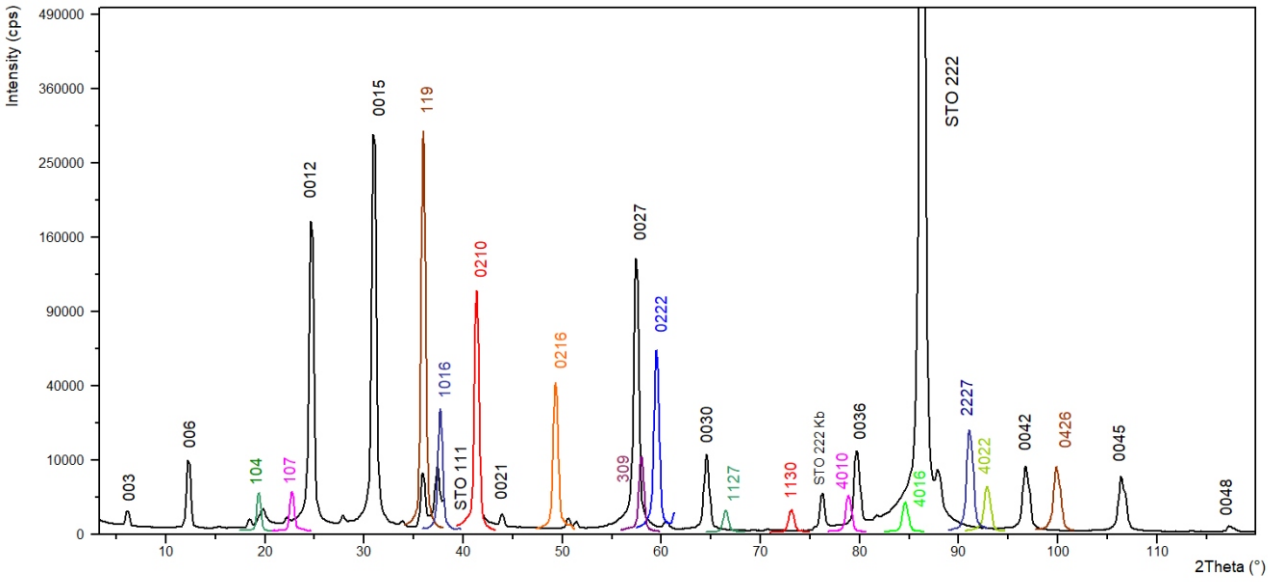

Figure 1. Powder-like diffraction pattern of Y-phase constructed from selected different peaks measured at specific angles of inclination and rotation by -2 scans (colors). 00*l* peaks and peaks from $SrTiO_3$ (STO) substrate were measured in symmetric -2 scan (black).

For the preparation of highly oriented ferrite films, several substrates were used, and different substrate/seeding layer/ferrite layer architectures were proposed [1]. The preparation of strongly oriented films appeared to be complicated for some of the phases.

The ME Z-type ferrite $Sr_3Co_2Fe_{24}O_{41}$ and $Ba_xSr_{3-x}Co_2Fe_{24}O_{41}$ thin films with strong out-of-plane and in-plane orientation were prepared and characterized for the first time [2]. In the former case, the analysis was complicated by the presence of M and S (spinel) phases that were also oriented (aligned with the substrate and one with another). Consequently, many weak asymmetric reflections were overlapped and careful selection of reflections suitable for the analysis had to be made. The magnetization data show anomalies in the magnetic behaviour occurring at temperatures close to the room temperature that are characteristic for collinear to noncollinear spin structure transitions. It was found that the ME effect can be stronger for the oriented film, but still with some disorder, than for a single crystal [3]. This effect should be verified yet.

The mechanism of ME effect in Y-phases may be a little different and it seems to be influenced significantly by lattice parameters. New Y-ferrite phases were prepared with the composition $Ba_xSr_{2-1}Co_2Fe_{11.1}Al_{0.9}O_{22}$, and it was found that the magnetic structure is of noncolinear ferrimagnetic type with an unspecified helical magnetic structure. These films could be prepared with good out-of-plane and in-plane orientation directly on STO - $SrTiO_3$(111) substrate, but M-phase seeding layer usually leads to better results. ME effect was identified to be maximum for x = 1 but its dependence on x is studied in more details now. In the project, we are investigating the influence of the degree and type of preferred orientation of the films as well as their real structure on the ME effect. By using different substrates, different preferred orientations and strains can be obtained.

XRD studies

In addition to symmetric Bragg-Brentano scans showing often only strong basal 00l diffractions, a combination of different scans to characterize both out-of-plane orientation and in-plane orientations were applied. The lattice parameters, profile analysis (crystallite size and strains), and residual stresses were studied by combination of several asymmetric reflections scanned at specific suitable angles of inclinations and azimuths [4], i.e. partially as for a single crystal. Example is shown on Fig. 1. Out-of-plane preferred orientation can be quickly estimated by the so-called -scans (rocking curves, rotation of sample at the fixed Bragg angle). Examples are shown on Fig. 2. In-plane orientation can be estimated by -scans, rotation of sample on the axis perpendicular to the surface for asymmetric (inclined to the surface) diffractions. Strong distinct peaks indicate alignment of the planes perpendicular to the surface with the substrate. Examples are shown on Fig. 3.

Overall picture can be provided also by fast reciprocal space mapping with 2D detector as described in [5] or in more details in [6]. 2D detectors are used without any secondary optics and the direction of the scattered beam is deduced only from the spatial position of a hit pixel. Angular resolution is given by the cross-section of the scattered beam, divergence of the primary beam and the solid angle covered by individual pixels. Therefore, the primary beam should have a small cross-section and should be well collimated horizontally and vertically. The detector can simultaneously measure the intensity of diffracted beams in different directions, i.e., it reveals the intensity distribution in continuous 2D area in reciprocal space without any movement. An appropriately chosen scan measures a set of neighboring 2D slices in reciprocal space. Such dataset when combined reveals the intensity distribution in 3D volume in reciprocal space.

The interpretation of the measured data can be qualitatively based on a direct observation such as a visibility of Debye rings, sensitivity of measured pattern on azimuth or

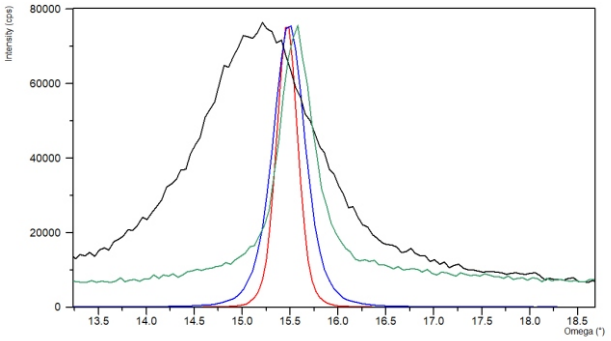

Figure 2. Out-of-plane orientation. -scans for different films of Y-phase, deposited on STO (111) - red, showing strong orientation, on $LaAlO_3$ (111) with M-phase seeding layer – blue, on STO (100) – green and on MgO (111) – black. The curves are roughly normalized to peak height. Higher background for green curve indicates significant amount of randomly oriented crystallites.

approximate width of partial Debye rings (Figure 4). The measured data can also be compared with the numerical simulation based on some expected model and the model parameters can be optimized to match the experimental data (Figure 5).

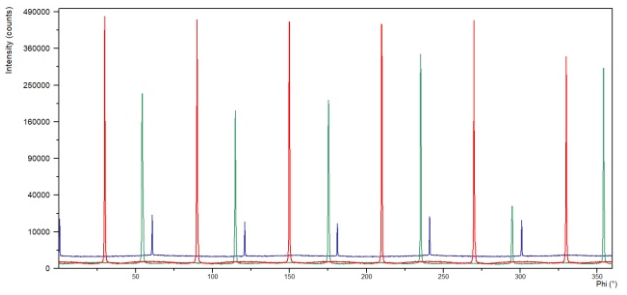

Figure 3a. In-plane orientation. -scans for different films of Y-phase on STO (111) substrate. All indicates good in-plane alignment but with different fraction of non-oriented crystallites.

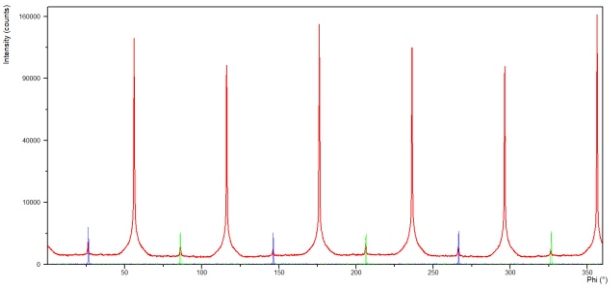

Figure 3b. In-plane orientation. -scans for Y-phase on $LaAlO_3$ (111) substrate with wide tails. -scans of substrate peaks are shown in blue (200) and green (220).

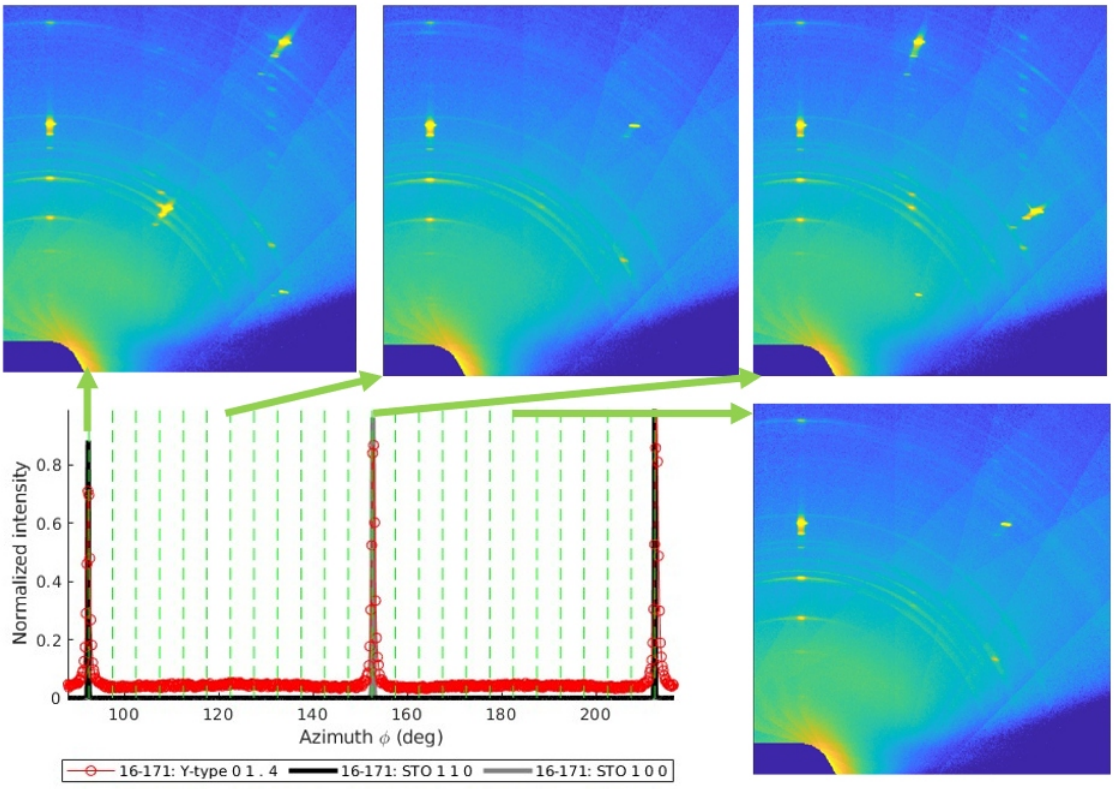

Figure 4. Parts of fast RSMs of Y-type hexaferrites taken at different azimuthal angles . The arrows indicate their correspondence to the positions in scans..In figures corresponding to the maxima in scans one can see the chains of diffractions of Y-phase (on the ight side). They can be simulated and shown on the picture (Fig. 5). It can also be seen that there is a fraction of completely randomly oriented grains, as it is indicated by the Debye rings.

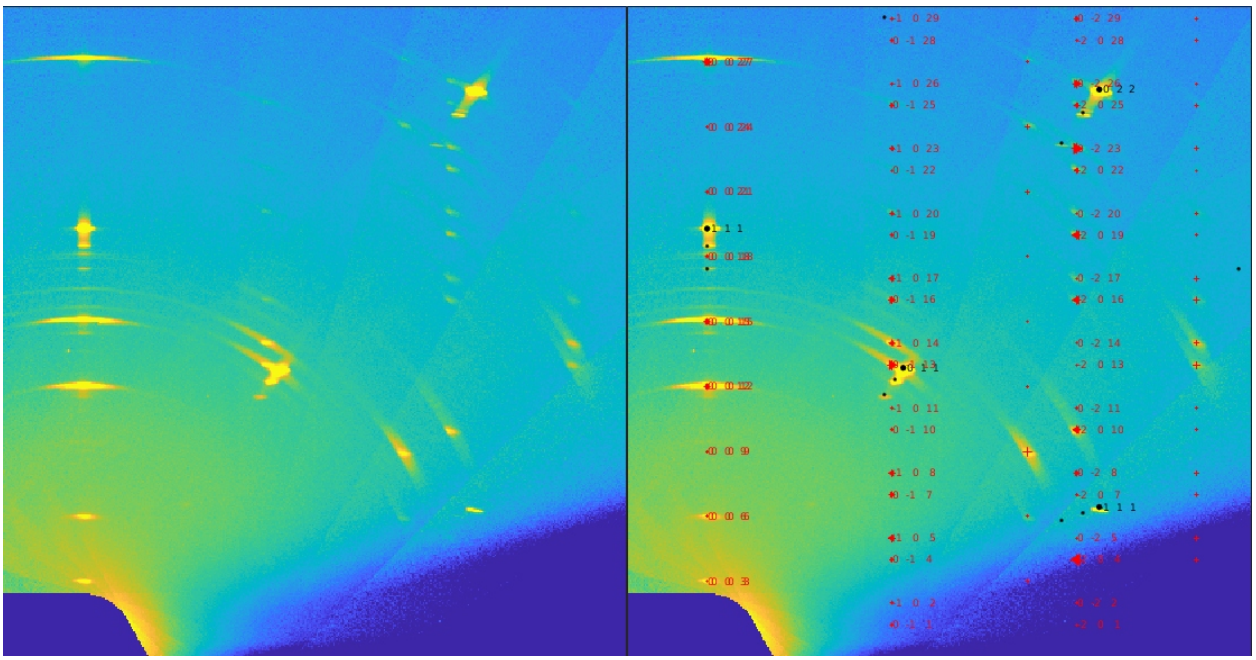

Figure 5. Example of fast RSM section of Y-type hexaferrites (on the left) with calculated positions of Y-phase diffractions.

1. R. Uhrecký, J. Buršík, M. Soroka, R. Kužel, J. Prokleška, *Thin Solid Films*, **622** (2017) 104-110.
2. J. Buršík, R. Uhrecký, M. Soroka, R. Kužel, J. Prokleška, *Journal of Magnetism and Magnetic Materials*, **469** (2019) 245-252.
3. Kwang Woo Shin, M. Soroka, Aga Shahee, Kee Hoon Kim, J. Buršík, R. Kužel, M. Vronka, M. Haydee Aguirre, *Advanced Electronic Materials*, (2022), 2101294.
4. R. Kužel, J. Čížek, M. Novotný, Metall. Mater. Trans. A (2013) 45–57. https://doi.org/10.1007/s11661-012-1432-x.
5. L. Horák, Materials Structure, vol. 27, no. 2 (2020) 98.
6. https://hal.science/hal-04058711/.

We acknowledge the support by Grant Agency of the Czech Republic no. GACR 24-12710S